



# Conjoint application of ultrasonication and redox pair mediated free radical method enhances the functional and bioactive properties of camel whey-quercetin conjugates

Waqas N. Baba, Raghad Abdelrahman, Sajid Maqsood\*

Department of Food Science, College of Agriculture and Veterinary Medicine, United Arab Emirates University, Al-Ain, 15551, United Arab Emirates

## ARTICLE INFO

### Keywords:

Bioactive  
Enzyme inhibition  
Techno-functional  
Whey-quercetin conjugation  
Ultrasonication

## ABSTRACT

Ultrasonication, redox-pair generated free radical method and their combination (Ultrasonication/redox-pair method) was used for production of camel whey-quercetin conjugates. FTIR and SDS-PAGE confirmed successful production of whey-quercetin conjugates using ultrasonication and ultrasonication/redox-pair method. FTIR suggested existence of covalent (appearance of new peak at  $3399\text{ cm}^{-1}$ ) and non-covalent linkages (shifting of peak at  $3271\text{ cm}^{-1}$ ,  $1655\text{ cm}^{-1}$  (amide I),  $1534\text{ cm}^{-1}$  and  $1422\text{ cm}^{-1}$  (Amide II)) in the whey-quercetin conjugates. Moreover, SDS-PAGE of conjugates produced by ultrasonication as well redox-pair method indicated shifting of protein bands slightly towards high molecular weight due to increase in the mass of proteins due to the binding of polyphenols. All conjugates showed improved techno-functional and bioactive properties in comparison to whey proteins. Conjugates produced through ultrasonication showed smaller particle size, improved solubility, emulsifying and foaming properties while conjugates produced through ultrasonication/redox-pair method depicted superior antioxidant properties in comparison to whey. Furthermore, conjugated samples showed higher inhibition of enzymatic markers involved in diabetes and obesity with highest potential recorded in conjugates produced using ultrasonication. Therefore, ultrasonication can be successfully used individually as well as in combination with redox-pair for production of whey-quercetin conjugates with enhanced bioactive and techno-functional properties.

## 1. Introduction

Conjugation of proteins with polyphenols is a research hot-spot in the field of food science due to diverse applications of protein–polyphenol conjugates in food industry. Proteins and polyphenols can associate through non-covalent as well as covalent interactions. Unlike non-covalent interactions, protein–polyphenol covalent interactions are very rare in nature and as such least studied. Covalent conjugation of polyphenol with whey protein molecules leads to the formation of a new-type of macromolecular that has enhanced techno functional and bioactive properties [5]. Covalent conjugation of proteins with polyphenols can be accomplished through different methods such as alkaline method, free radical method, enzymatic method, and chemical coupling. Among these methods' covalent conjugation by free radical mediated method is preferred due to economic and non-toxicity considerations. Successful grafting of various polyphenols with different proteins using free radical approach has been reported with improved

functional and antioxidant properties [38]. Free radical method involves use of a redox-pair such ascorbic acid/ $\text{H}_2\text{O}_2$  to generate free radicals that mediate the reaction between proteins and polyphenols. However, the industrial application of redox-pair mediated free radical method to produce protein–polyphenol conjugates is limited by various drawbacks such as low degree of conjugation and high reaction time [26]. Xu et al. [64] recently reported that ultrasonication can be successfully used for grafting soy-protein isolates with cyanidin-3-galactoside. However, there is very scarce literature related to the utilization of ultrasonication on the production of protein–polyphenol conjugates. Recently ultrasonication was reported to improve the conjugation of tea polyphenols with egg white proteins when coupled with alkaline method of conjugation [26]. Also, ultrasonication was reported to improve the binding of allicin to whey proteins [24]. However, to the best of our knowledge there is no existing literature that reports use of ultrasonication for production of whey-quercetin conjugates. Furthermore, there is no study that compares ultrasonication with the redox-pair method and

\* Corresponding author.

E-mail address: [sajid.m@uaeu.ac.ae](mailto:sajid.m@uaeu.ac.ae) (S. Maqsood).

<https://doi.org/10.1016/j.ultsonch.2021.105784>

Received 22 June 2021; Received in revised form 16 August 2021; Accepted 26 August 2021

Available online 8 October 2021

1350-4177/© 2021 The Author(s).

Published by Elsevier B.V. This is an open access article under the CC BY-NC-ND license

(<http://creativecommons.org/licenses/by-nc-nd/4.0/>).

their combination to produce whey-polyphenol conjugation.

Whey proteins due to their versatile functionality have been used in different food formulations such as ice creams, beverages, baked products infant formulae [30]. Despite of being a rich source of essential amino acids with high bioavailability and therapeutic properties, its use in food industry is limited due to its deterioration during processing. Denaturation induced due to thermal and pH variation during processing not only results in precipitation and turbid appearance of whey proteins but also induces formation of protein network that make processing a difficult task [39]. To overcome these drawbacks various methods have been used to modify whey for improved use in food industry. Recently, production of modified whey-polyphenol conjugates with enhanced techno-functional as well as bioactive properties is generating high research interest and has been identified as the hotspot in the field of food science [13]. Moreover, recent research on whey proteins from camel milk is gaining considerable importance in today's world due to its therapeutic properties [3,6,7]. Camel whey has been reported for their high techno-functional potential that warrants its use in food industry [32,33,68]. Camel whey proteins differ from bovine whey due to the absence of beta-lactoglobulin [40] and consists of higher amounts of lactoferrin ( $pI = 8.63$ ), serum albumin ( $pI = N.A.$ ) and  $\alpha$ -lactoalbumin ( $pI = 4.87$ ) [18] compared to bovine whey. Laleye et al. [34] reported that camel whey proteins were less soluble and more heat sensitive than bovine whey with least solubility at a pH of around 4.5. The heat sensitive and less soluble nature of camel whey in comparison to cow whey has been attributed to absence of  $\beta$ -lactoglobulin that makes its utilization in food industry an uphill task. Camel whey was reported to have higher emulsifying activity index and surface hydrophobicity than bovine whey while its emulsifying stability index was inferior. Moreover, lack of efficient techniques and under-investigated status of camel whey limits its full-scale utilization in food industry.

Considering recent developments and existing gaps, this study was designed to compare ultrasound and redox-pair (Ascorbic acid/ $H_2O_2$ ) mediated free radical method for production of camel whey-quercetin conjugates. The conjugates produced were characterized and studied for techno-functional and bioactive properties. Furthermore, most of the bioactivities of whey protein-polyphenol conjugates till date have been confined to antioxidant properties only. To the best of our knowledge the *in-vitro* antidiabetic and anti-obesity potentials of any fabricated protein-polyphenol conjugate have not been reported till date. As such the effect of conjugation of whey with polyphenol on inhibition of key enzymatic markers involved in diabetes and obesity was also compared.

## 2. Material and methods

Chemicals and reagents required for SDS-PAGE (Richmond, CA) were procured from Sigma Aldrich (St. Louis, MO, USA). Quercetin, 2,2-diphenyl-1-picrylhydrazyl (DPPH), 2,2'-azino-bis (3-ethylbenzothiazoline-6-sulfonic acid (ABTS), pancreatic  $\alpha$ -amylase (VI-B  $\geq 5$  units/mg of solid), and yeast  $\beta$ -glucosidase (type I, lyophilized powder  $\geq 10$  units/mg of protein), ascorbic acid,  $H_2O_2$  and rest of the chemicals were procured from Sigma Aldrich (St. Louis, MO, USA). All the chemicals used in the study were of analytical grade and were used without any further purification.

### 2.1. Production of whey-quercetin conjugates

Freeze dried camel whey was produced in the laboratory of Dept. of Food Science, United Arab Emirates University (UAEU) as per the method described by Baba et al. [7]. A 20% solution of freeze-dried whey was subjected to dialysis using a dialysis tubing (SnakeSkin®, Thermo Fisher Scientific) with 3.5 KDa molecular weight cut off (MWCO) for 48 h at 4 °C to remove salts and lactose followed by freeze drying. Three different methods with some modifications were used to produce conjugates: redox-pair method [56], ultrasonication [64] and a conjoint use of ultrasonication and redox-pair method (ultrasonication/

redox-pair method).

#### 2.1.1. Redox-mediated whey-quercetin conjugate

Redox-pair consisting of 1 g of ascorbic acid and 4 mL of  $H_2O_2$  (5 mM) were added to aqueous whey solution (2 g /100 mL). After storing the solution for 2 h to allow generation of free radicals, quercetin (1 g /5 mL of DMSO) was added to ensure a protein: polyphenol ratio of 1:0.5. This ratio has been reported to achieve maximum conjugation of polyphenol with protein as reported in case of  $\beta$ -LG-chlorogenic acid conjugates [15]. The reaction mixture was stored at room temperature for 24 h that served as redox-mediated whey-quercetin conjugate (PR).

#### 2.1.2. Ultrasonication

Another two groups of whey-quercetin conjugates with and without redox-pair were also synthesized using ultrasonication. The reaction mixture was prepared as mentioned above but instead of storing for 24 h, it was immediately ultrasonicated at time 30 and 60 min. Ultrasonication (Branson 550, Danbury, USA) was carried out using a tapered Microtip titanium probe (3.2 mm) in pulsed mode with 30 s off cycle, amplitude 70% that generated a power of 150 W. Samples (200 mL) were immersed in the ice bath during the ultrasonication process to ensure that the temperature did not exceed 30 °C. Whey solution (1 g/100 mL) served as control.

The resulting solution were labelled as:

Whey: Control solution of whey protein.

PR: Whey with redox pair only.

PUS1: Reaction mixture without redox-pair & ultrasonicated for 30 min

PUS2: Reaction mixture without redox-pair & ultrasonicated for 60 min

PRUS1: Reaction mixture with redox-pair & ultrasonicated for 30 min

PRUS2: Reaction mixture with redox-pair & ultrasonicated for 60 min

Quercetin: Control solution of quercetin

All the whey-quercetin conjugates viz, PR, PUS1, PUS2, PRUS1, PRUS2 were again subjected to dialysis using a dialysis tubing (Snake-Skin®, Thermo Fisher Scientific) with a 3.5 KDa molecular weight cut off (MWCO) for 48 h with 8 changes in water to remove undissolved quercetin. The samples were further centrifuged at 3000g for 15 min to ensure removal of undissolved quercetin. Samples were prepared in triplicates and further divided into two sets: a liquid set for determining surface hydrophobicity, particle size, zeta potential, emulsion and foaming capacity while another was freeze dried for rest of the analyses.

### 2.2. Characterization of whey-quercetin conjugates

#### 2.2.1. UV-Vis spectroscopy

All the samples (0.05 mg/mL) were subjected to UV-vis spectroscopy from 200 to 800 nm (SkanIt, Thermofisher). Two different solvents were used because pure quercetin (control) is sparingly soluble in water .

#### 2.2.2. SDS-Page

All whey-polyphenol conjugate samples and control were characterized using SDS-PAGE under reducing condition as described by Maqsood et al. [40], with slight modifications. Samples were characterized under reducing conditions using a 12% acrylamide-bis acrylamide solution (resolving gel) and 4% stacking gel. Samples were run using a Mini Protean III apparatus (Bio-Rad, Techview, Singapore) having a gel size of  $7 \times 8 \text{ cm} \times 0.75 \text{ mm}$ . Before loading 10  $\mu\text{L}$  of sample onto the gel, sample and sample buffer (12% glycerol; 1.2% SDS; 5.4%  $\beta$ -mercaptoethanol; bromophenol blue) at a ratio of 2:1 was boiled at 100 °C for 3 min. Coomassie Blue stain was used for visualizing the gel. Electrode buffer (1L) used consisted of 3 g of Tris, 14.4 g of glycine and

1 g of SDS in distilled water (pH 8.3). Electrophoresis was performed at constant current of 15 mA for each gel.

### 2.2.3. Total flavonoid content (TFC)

The total flavonoid content of samples was determined as per the method described by Herald et al. [19]. Briefly, 25  $\mu$ L of each sample was added to the microplate followed by addition with 100  $\mu$ L of distilled water and 10  $\mu$ L of NaNO<sub>2</sub> (50 g/L). The reaction mixture was allowed to react for 6 min followed by addition of 15  $\mu$ L AlCl<sub>3</sub> (100 g/L), 50  $\mu$ L NaOH (40 g/L) and 50  $\mu$ L of distilled water. After 30 s of shaking, absorbance was taken at 510 nm in a microplate reader (Multiskan Sky, ThermoFisher). Sample blank was run to remove the interference from sample. A standard curve ( $r^2 = 0.994$ ) of quercetin (10–1000  $\mu$ g/mL) was used to calculate the TFC content of samples and expressed as  $\mu$ g quercetin equivalent per gram of the sample ( $\mu$ g QE/g).

### 2.2.4. Fourier transform Infra-red spectroscopy (FTIR)

FTIR spectra of whey-quercetin conjugates was recorded using ATR-FTIR spectrophotometer (Spectrum Two UATR, PerkinElmer, UK) as described by Ahmad et al. [1]. Freeze dried samples were placed on the ATR crystal and the spectra was collected in the wave number ranges of 400–4000  $\text{cm}^{-1}$ .

### 2.2.5. Particle size and zeta potential

The particle size distribution and zeta potential of samples was determined directly after production of conjugates when the particles were still dispersed in the collection fluid. An aliquot from each sample was diluted (1:100) with deionized water to reach a proper intensity as required by the equipment (NanoPlus DNS, Micromeritics, USA). The analysis was carried out at a temperature of 25.0 °C and refractive index of 1.3328 (water) was selected. The particle size and zeta potential were generated using inbuilt software.

### 2.2.6. Surface hydrophobicity

Surface hydrophobicity was determined according to the method of Chelch et al. [12] with slight modifications. Briefly, 1 mL of each sample (1 mg/mL) was mixed with 200  $\mu$ L of bromophenol blue (BPB) (1 mg/mL) and vortexed. Control consisted of similar volume except for sample replaced with tris-HCl buffer (20 mM, pH 8). The reaction mixture was shaken for 10 min at room temperature and centrifuged for 15 min at 2000 g. The supernatant was diluted with deionized water (1:10) and absorbance was measured at 595 nm. The amount of BPB bound was measured using equation below. Greater the BPB content means higher surface hydrophobicity.

$$\text{Amount of BPB bound}(\mu\text{g}) = \frac{(A_c - A_s)}{A_c} \times 200\mu\text{g}$$

where  $A_c$  is the absorbance of control and  $A_s$  is the absorbance of sample

## 2.3. Functional properties

### 2.3.1. Protein solubility

Freeze dried samples (1 mg/ml) were suspended in water (1 mg/mL), centrifuged at 12,000g for 30 min and the supernatant was analyzed for protein content using the Bicinchoninic acid assay method. Aliquot (25  $\mu$ L) from supernatant of each sample was added to working reagent that consisted of Reagent A (bicinchoninic acid) and Reagent B (cupric sulphate) in the ratio of 50:1. Aliquot and working reagent were mixed in the ratio of 1:8. The reaction mixture was incubated at 37 °C for 30 min and analyzed at 562 nm. Bovine serum albumin was used as standard for calculating the protein content using equation ( $y = 0.0007x + 0.1312$ ;  $r^2 = 0.9943$ ).

### 2.3.2. Foaming property

The foaming properties of whey-quercetin conjugates was deter-

mined as described by Li et al. [36]. Approximately 20 mL of the liquid sample was homogenized (Ultra Turaxx, T 25, Germany) in a 50 mL graduated cylinder at 10000 rpm for 90 s using a high shear mixer to generate a foam. The foaming capacity and foaming stability of samples was calculated using the formulae:

$$\text{Foaming capacity}(\%) = \frac{V_2}{V_1} \times 100$$

$$\text{Foaming stability}(\%) = \frac{V_f}{V_2} \times 100$$

where  $V_1$  is the initial volume before shearing,  $V_2$  is the volume of the foam after shearing and  $V_f$  volume of the foam 60 min after shearing.

### 2.3.3. Emulsifying property

Oil-in-water emulsion was made by homogenizing sunflower oil and water in the ratio of 1:3 at a speed of 10,000 rpm for one minute. The emulsion was pipetted out at 0 and 10 min followed by 100 times dilution with SDS (1 mg/mL) solution. Absorbance was determined by spectrophotometer (Multiskan Sky, ThermoScientific, Finland) at 500 nm. The emulsification activity index (EAI) and emulsion stability index (ESI) were calculated as follows:

$$\text{Emulsion activity index}(\text{m}^2/\text{g}) = \frac{2 \times 2.303 \times A_0 \times DF}{\rho \times \varphi \times \theta \times 10000}$$

$$\text{Emulsion stability index}(\%) = \frac{A_{10}}{A_0} \times 100$$

## 2.4. Antioxidant activity

### 2.4.1. DPPH radical scavenging activity

DPPH radical scavenging activity was performed as described by Baba et al. [4] with some modifications. Briefly, 150  $\mu$ L of each sample (1 mg/ml) (Hepes buffer pH = 7.5, 0.1 M) was mixed with 150  $\mu$ L DPPH (0.15 mM) in ethanol and incubated for 30 min and the absorbance was measured at 517 nm and DPPH radical scavenging activity was expressed in terms of quercetin equivalent antioxidant capacity (QEAC) per mg of sample by comparing IC<sub>50</sub> value of quercetin to IC<sub>50</sub> value of sample (IC<sub>50</sub> of quercetin / IC<sub>50</sub> of sample). The IC<sub>50</sub> value of sample was calculated by plotting different concentrations of sample while the IC<sub>50</sub> value of quercetin was calculated from a quercetin standard curve ( $r^2 = 0.986$ ) produced by using different concentrations of quercetin (5–200  $\mu$ g/ml). **ABTS radical scavenging activity**

ABTS working reagent was prepared by mixing ABTS solution (0.014 M) and K<sub>2</sub>S<sub>2</sub>O<sub>8</sub> (0.0048 M) in a ratio of 1:1 in an amber bottle and allowed to react for 12 h. The solution was diluted 100 times with methanol to achieve an absorbance below 1. Briefly 30  $\mu$ L of each sample (1 mg/ml) (Hepes buffer pH = 7.5, 0.1 M) was mixed with the 270  $\mu$ L ABTS working reagent and incubated for 2 h in dark. Trolox served as standard and was used to obtain the IC<sub>50</sub> value. The absorbance was taken at 734 nm. quercetin equivalent antioxidant capacity (QEAC) per mg of sample by comparing IC<sub>50</sub> value of quercetin to IC<sub>50</sub> value of sample (IC<sub>50</sub> of quercetin / IC<sub>50</sub> of sample). The IC<sub>50</sub> value of quercetin and samples was calculated by plotting different concentrations of sample concentration while the IC<sub>50</sub> value of quercetin was calculated using a quercetin standard curve ( $r^2 = 0.991$ ) produced using different concentrations of quercetin (5–200  $\mu$ g/ml).

## 2.5. In-vitro antidiabetic and anti-obesity properties

### 2.5.1. $\alpha$ -Glucosidase inhibition (AGI) and DPP-IV inhibition (DI)

The AGI inhibition activity of conjugates was determined according to the method described by Baba et al. [7] with slight modifications. Briefly, 50  $\mu$ L of each sample (5  $\mu$ g/mL) was mixed with 100  $\mu$ L of enzyme (0.2 U/mL) in 50  $\mu$ L of Hepes buffer (0.1 M, pH = 6.8). The

mixture was incubated at 37 °C for 10 min followed by addition of p-nitrophenol- $\beta$ -D-glucopyranoside (*p*-NPG) (10 mM). The mixture was incubated for 30 min at 37 °C and the absorbance was measured at 405 nm.

The DPP-IV inhibitory activity of the conjugates was determined according to the method described by Kamal et al. [27] with slight modifications. Briefly 50  $\mu$ L of sample (5  $\mu$ g/ml) was mixed with 50  $\mu$ L of enzyme (0.01  $\mu$ g/mL) in 50  $\mu$ L of HEPES buffer (0.1 M, pH = 8.0). The mixture was incubated at 37 °C for 10 min followed by addition 50  $\mu$ L of GLY-PRO-Paranitro anilide (500  $\mu$ M). The mixture was incubated for 30 min at 37 °C and the absorbance was measured at 405 nm.

The percentage inhibition of enzyme markers was calculated using equation:

$$\% \text{inhibition} = \left[ \frac{A_c - A_s}{A_c} \right] \times 100$$

where  $A_c$  is the absorbance of control and  $A_s$  is the absorbance of sample obtained after subtracting the sample blank (all the reagents except enzyme).

### 2.5.2. Cholesterol esterase and pancreatic lipase inhibition

Cholesterol esterase inhibition (CEI) was determined according to the method described by Jafar et al. [20] with slight modification. The CWPHs were incubated with a substrate (50  $\mu$ L) containing 5 mM p-

nitrophenyl butyrate in 100 mM sodium phosphate buffer, and 100 mM NaCl in a 96-well microtiter plate. About 50  $\mu$ L of porcine pancreatic CE (5  $\mu$ g/mL) was added to each well and incubated at 37 °C for 30 min. The *p*-nitrophenol released from enzymatic hydrolysis of *p*-nitrophenyl butyrate was spectrophotometrically determined at 405 nm using a microplate reader.

Pancreatic lipase inhibition (PLI) was determined according to the method described by Jafar et al. [20]. Briefly, 50  $\mu$ L of sample was mixed with pancreatic lipase (20  $\mu$ L) and *p*-nitrophenyl butyrate (25  $\mu$ L) in HEPES buffer (pH = 7.4) in a 96 well microplate reader. Using HEPES buffer the reaction mixture was raised to 150  $\mu$ L. The reaction mixture was incubated at 37 °C for 30 min. Each sample based on its inhibiting potential decreased the generation of *p*-nitrophenyl that was recorded at 405 nm in a microplate reader.

The percentage inhibition of enzyme markers was calculated using equation:

$$\% \text{inhibition} = \left[ \frac{A_c - A_s}{A_c} \right] \times 100$$

where  $A_c$  is the absorbance of control and  $A_s$  is the absorbance of sample obtained after subtracting the sample blank (all the reagents except enzyme).

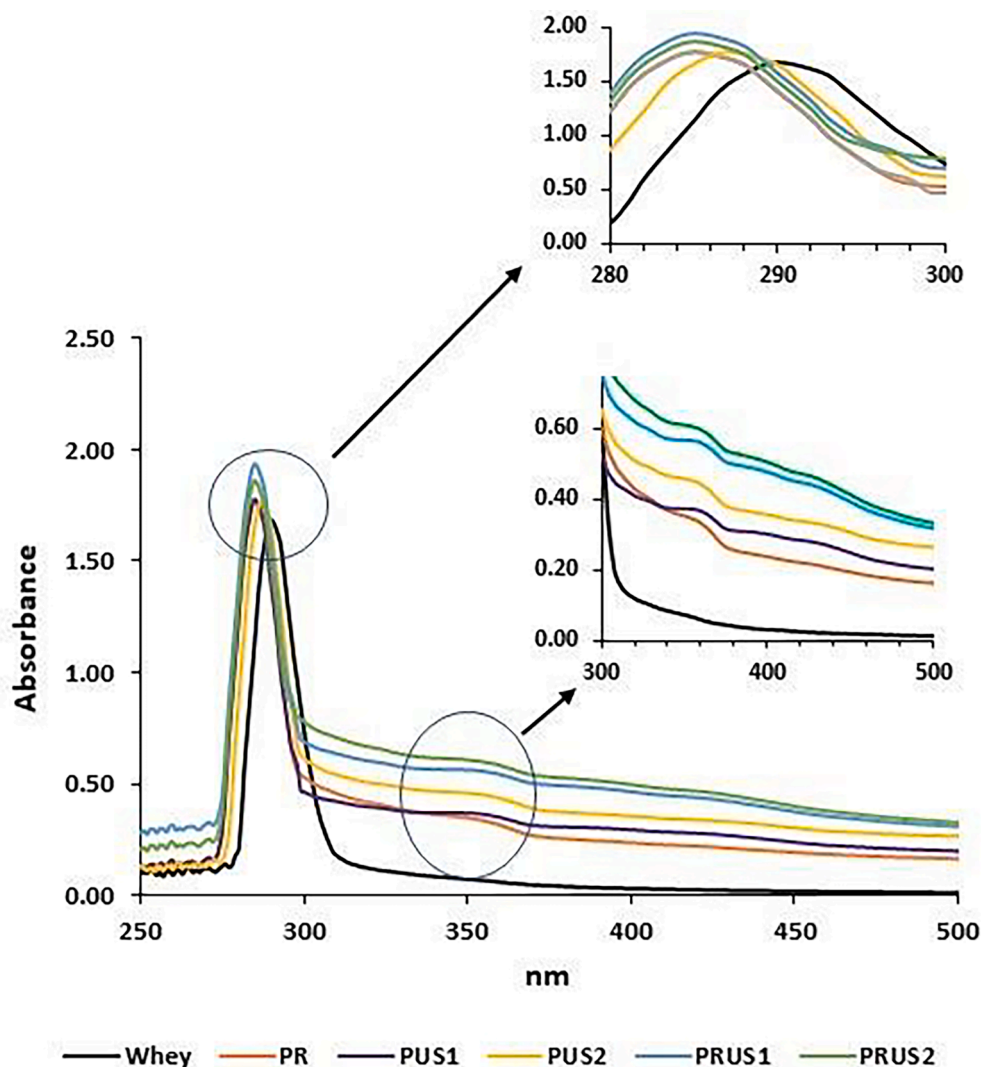


Fig. 1. UV-Vis spectrum of camel whey and its conjugates with quercetin produced using redox pair method and ultrasonication.

## 2.6. Statistical analysis

Statistical analysis was carried out using Minitab version 20. All the experiments were done in triplicates and the data obtained was analyzed using two-way ANOVA. To obtain significant difference between different means, means were compared using Tukey test at a 95% level of significance ( $P < 0.05$ ).

## 3. Results and discussion

### 3.1. Characterization of conjugates

#### 3.1.1. UV-vis spectroscopy

The UV-vis spectrum of whey, pure quercetin and whey-quercetin conjugates is depicted in Fig. 1. Whey showed a characteristic peak at 280 nm that is attributed to aromatic amino acids such as tyrosine, tryptophan and phenylalanine present in whey. After conjugation with quercetin, a bathochromic shift as well as increase in the absorbance values was recorded. In addition, the experimental data was supported by the visual appearance of the conjugates that resulted in bright yellow-orange colored aqueous solutions suggesting enhanced solubility of quercetin. Evidently when quercetin (0.05 mg/ml of water) was scanned as control, no prominent peak could be detected that was supported by visible examination also (solution was colorless due to insolubility of quercetin) (Fig. 1). Additionally, for determining the lambda max of quercetin, an ethanolic solution of quercetin (0.05 mg/ml) was analyzed through UV-Vis spectroscopy showing the characteristic peak of quercetin at 370 and 250 nm (Supplementary material Fig S1).

Increased absorbance at 280 nm of whey-quercetin conjugates can be attributed to binding of quercetin with whey while the bathochromic shift in the peak absorbance suggests quercetin interacted with the aromatic amino acid present in whey resulting in a change in the micro-environment surrounding the whey chromophores. Whey-quercetin conjugates could be differentiated from whey by the presence of a hump around  $\approx 350$  nm (absent in whey sample) that can be attributed to quercetin binding to whey protein. For better resolution, the second derivative of the spectrum is presented (supplementary material Fig S2) which displayed peaks (380 and 420 nm) found in conjugates revealing

a distinctive feature in all the conjugates except PR. These additional peaks in samples that were produced using ultrasonication and/or ultrasonication/redox-pair method may be attributed to presence of both covalently and non-covalently linked quercetin.

#### 3.1.2. SDS-Page

SDS-PAGE of camel whey showed presence of major whey proteins such as serum albumin, lactoferrin and  $\alpha$ -lactalbumin ( $\alpha$ -LA) as previously reported [40]. Conjugation of whey with polyphenols showed a visible effect (shifting and less intense of protein bands) that varied depending on the method of conjugation (Fig. 2). The treatments resulted in shifting of protein bands slightly towards high molecular weight due to increase in the mass of proteins as a result of binding of polyphenols. Wu et al. [61] reported migration of  $\beta$ -lactoglobulin (BLG) protein band slightly towards high molecular weight in SDS-PAGE of  $\beta$ -LG-epigallocatechin gallate/chlorogenic acid conjugates which indicates successful covalent conjugation. Similar trend was reported by Yi et al. [65] after covalent conjugation of  $\alpha$ -LA and catechin. The SDS breaks only non-covalent linkages without affecting the covalent bonds. Thus, the stability of the whey-polyphenol complex indicated by high molecular mass (Lane 2) during SDS-PAGE suggests whey was covalently linked to polyphenols in whey-polyphenol conjugate. Despite of higher flavonoid content (discussed in next section) of PUS1, inconspicuous difference in shifting of bands was seen in PUS1 compared to PR. This might be due to the presence of higher fraction of non-covalently linked quercetin using ultrasonication leading to higher flavonoid content. Ultrasonication was reported to generate soy-protein-cyanidin-3-galactoside conjugates linked by covalent as well as non-covalent linkages [64]. Moreover, same quantity of each sample (weight basis) was analyzed for SDS-PAGE, each containing varying levels of conjugated quercetin that decreased the protein concentration on compositional basis resulting in less intense protein bands in conjugates. Fading of protein bands in SDS-PAGE analysis of whey conjugates with epigallocatechin-3-gallate (EGCG), gallic acid [9] and quercetin [45] was attributed to the higher intermolecular cross linking with the polyphenol. A careful examination of SDS-PAGE of PUS2 in comparison to PUS1 showed more intense bands near high molecular weight whey proteins that can be attributed to protein aggregation of whey protein

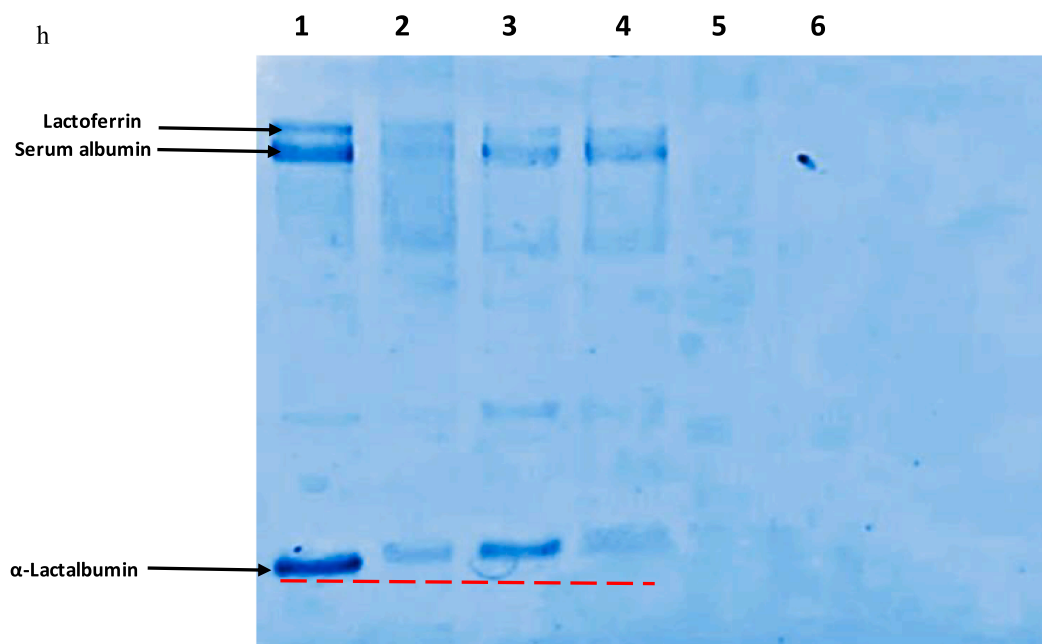


Fig. 2. SDS-PAGE of camel whey (Lane 1) and its conjugates with quercetin prepared using Lane 2: Redox-pair (PR); Lane 3: Ultrasonication for 30 min.; Lane 4: Ultrasonication for 60 min.; Lane 5: Ultrasonication/redox-pair for 30 min.; Lane 6: Ultrasonication/redox-pair for 60 min.

molecules due to prolonged ultrasonication. This is in consent to the results of particle size analysis in this study (Table 1). Similar results were reported in high molecular weight proteins of whey during ultrasonication for 20 min [29]. However, bands attributed to  $\alpha$ -LA (Lane 4) corresponding to US2 showed decreased intensity in comparison to  $\alpha$ -LA bands (Lane 3) corresponding to US1 suggesting affinity of  $\alpha$ -LA towards quercetin as less intense bands were associated with higher conjugation with quercetin. Jambrak et al. [22] reported that higher ultrasound treatment time from 15 to 30 min resulted in a decrease of molecular weight of proteins due to breaking down of protein chains. Notably, a combination of ultrasonication and redox pair for conjugation results in complete disappearance of protein bands that might be due to excessive generation of free radicals resulting in high level of conjugation as well as possibility of protein chain breakdown. Thus, treatment of ultrasonication can be successfully used for conjugation of quercetin with whey proteins.

### 3.1.3. Total flavonoid content (TFC)

The total flavonoid content of conjugates was determined to know the quantity of quercetin that had conjugated with the whey proteins. The TFC content was lowest in PR (76  $\mu$ g QE/mg) that increased significantly ( $\approx$ 2 times) in conjugates (PUS1 = 136  $\mu$ g/mg & PUS2 = 162  $\mu$ g/mg) produced using ultrasonication (Fig. 3). Jiang et al. [24] also confirmed production of Allicin-whey protein conjugates using ultrasonication. Ultrasonication generates free radicals by cavitation as well as denatures the protein exposing hydrophobic sites, thereby facilitating both covalent as well as non-covalent binding of a hydrophobic flavonoid to whey protein. Recently, ultrasonication was reported to induce conjugation between soy proteins and cyanidin-3-galactoside through covalent as well as non-covalent linkages [64]. Highest TFC was seen in conjugates (PRUS1 = 187  $\mu$ g/mg & PRUS2 = 205  $\mu$ g/mg) produced using ultrasonication /redox-pair method. A higher level of conjugation between egg white protein and Proanthocyanidins by conjoint application ultrasonication with redox-pair method as well as alkaline method was recently reported in egg white protein [26]. Thus, ultrasonication and ultrasonication/redox-pair method can be used to produce conjugates with higher flavonoid content in comparison to redox-pair mediated conjugation.

### 3.1.4. FTIR

FTIR (Fig. 4a) of camel whey showed prominent peaks at 3271.72  $\text{cm}^{-1}$  (peak 1; amide A region), 2899.96  $\text{cm}^{-1}$  (peak 2), 1655 (peak 3, Amide I) and 1534 (peak 4, Amide II) as previously reported in camel whey [2]. While peak 1, 2 and 4 showed a spectral shift [13] (Supplementary material; Table S1), peak 2 completely disappeared after conjugation of whey with quercetin. Both ultrasonication and redox-pair fabricated conjugates showed emergence of a new peak around 3398  $\text{cm}^{-1}$  (Fig. 4 c, d). Jia, Zheng, Tao, Chen, Huang, & Jiang, [23] confirmed emergence of this peak and attributed it to covalent conjugation of whey proteins to EGCG using alkaline method. Notably the area under this peak was higher in conjugates fabricated using ultrasonication in comparison to PR suggesting higher level of conjugation.

**Table 1**

Particle size, solubility, zeta potential and surface hydrophobicity of camel whey-quercetin conjugates.

Sample	Particle size (nm)*			Poly disparity Index	Solubility (%)	Zeta potential	Surface hydrophobicity
	D10	D90	Average Diameter				
Control	402.5	736.2	561.3 $\pm$ 167.3	0.311	61.14 $\pm$ 0.01 <sup>f</sup>	-26.9 $\pm$ 0.5 $\pm$ 0.01 <sup>f</sup>	181.29 $\pm$ 5.98 <sup>a</sup>
PR	139.1	236.4	188.7 $\pm$ 52.6	0.615	72.29 $\pm$ 0.01 <sup>d</sup>	-55.5 $\pm$ 0.2 $\pm$ 0.01 <sup>d</sup>	163.20 $\pm$ 2.52 <sup>b</sup>
PUS1	47.4	83.4	65.5 $\pm$ 21.4	0.271	79.36 $\pm$ 0.00 <sup>c</sup>	-59.8 $\pm$ 0.3 $\pm$ 0.01 <sup>c</sup>	127.67 $\pm$ 3.06 <sup>d</sup>
PUS2	88.4	154.3	121.2 $\pm$ 57.9	0.372	66.41 $\pm$ 0.01 <sup>e</sup>	-52.8 $\pm$ 0.2 $\pm$ 0.01 <sup>e</sup>	141.52 $\pm$ 1.72 <sup>c</sup>
PRUS1	30.5	40.4	47.5 $\pm$ 293.5 <sup>#</sup>	0.484	82.47 $\pm$ 0.01 <sup>b</sup>	-71.9 $\pm$ 0.5 $\pm$ 0.01 <sup>a</sup>	106.01 $\pm$ 2.30 <sup>e</sup>
PRUS2	55.9	93.8	75.0 $\pm$ 19.9	0.383	90.72 $\pm$ 0.04 <sup>a</sup>	-67.3 $\pm$ 0.4 $\pm$ 0.01 <sup>b</sup>	102.59 $\pm$ 1.86 <sup>e</sup>

\* Supplementary files for graphs and detailed information.

# SD was high due to bimodal distribution of the particles (See supplementary material).

The peak shifting and change in the area of various peaks along amide A, amide I, amide II and amide III region of camel whey may also be attributed to conjugation with quercetin (Supplementary material; Table S1). To be precise peak 3271  $\text{cm}^{-1}$  (whey) shifted to 3267 (PR), 3270 (PUS1), 3275.1 (PUS2), 3270 (PRUS1) and 3277 (PRUS2)  $\text{cm}^{-1}$  respectively. Furthermore, peak 1655 (Amide I region), 1534 and 1422  $\text{cm}^{-1}$  (Amide II) shifted to 1658, 1520 and 1449  $\text{cm}^{-1}$ . The shifting of peaks in amide I and amide II regions was also reported during covalent and non-covalent association of EGCG [61] and chlorogenic acid [25] with whey proteins, respectively. This shifting of bands is attributed to structural changes induced in the protein after linking with polyphenols. The area swept by peak 1 (attributed to the intermolecular bonded -OH stretching) increased by 55.11, 129.47, 102.70, 132.21, 119.48 % in P1R, P1US1, P1US2, P1RUS1, P1RUS2, respectively (Supplementary material Table S1). The increased area swept by peak 1 may be because of non-covalent incorporation of quercetin. Evidently, ultrasonicated conjugates showed markedly higher % increase in the area suggesting increased hydrogen bonding that might be due to linking of quercetin to whey through hydrogen bonding (Supplementary Material; Fig S3). Notably, the results support the TFC values obtained in this study where a higher TFC content in the conjugates produced using US was reflected in the inconspicuous shifting of proteins band ( $\alpha$ -LA) towards higher molecular weight as seen in SDS-PAGE (a measure of lesser covalently bonded quercetin). These results support the outcome of previous studies where existence of both covalent as well as non-covalent linkages in soy-cyanidin conjugates produced using ultrasonication were reported [64]. An increase in the ultrasonication time decreased the area under peak 1 that might be due to mechanical stress caused by sonication for longer time. Furthermore, area under Peak 3 in the region 1650–1660  $\text{cm}^{-1}$ , associated with the  $\alpha$ -helical  $2^\circ$  structure of  $\alpha$ -LA [42] and albumin [11] decreased from 743.23 (whey) to 633.71 (PR), 461.18 (PUS1), 246.18 (PUS2), 464.83 (PRUS1), 439.77 (PRUS2). Also, Peak 3 migrated from 1655.73 in whey to 1658.71 (PR), 1658.29 (PUS1), 1660.67 (PUS2), 1660.93 (PRUS1), 1661.59 (PRUS2) that might be related to the structural changes and new bonds formed after conjugation. Thus, ultrasonication and ultrasonication/redox-pair method can be successfully employed for conjugation of quercetin with whey proteins more efficiently than redox-pair mediated method of conjugation.

### 3.1.5. Particle size

The particle size of all the conjugates was lower than unmodified whey proteins irrespective of the method of production (Table 1). A detailed information related to number distribution (graph and tables) of control whey and its conjugates is presented as Supplementary Material. Decrease in particle size can be attributed to decreased hydrophobicity due to increased hydroxyl groups in whey-quercetin conjugates that may prevent the aggregation resulting in smaller particle size. Conjugation of lactoferrin with EGCG was reported to introduce steric hinderances that prevented aggregation of lactoferrin [37]. The particle size of soy protein isolates also decreased after covalent conjugation with anthocyanins using ultrasonication [64]. However, particle size of PUS2 was significantly higher than PUS1. Increase in particle size

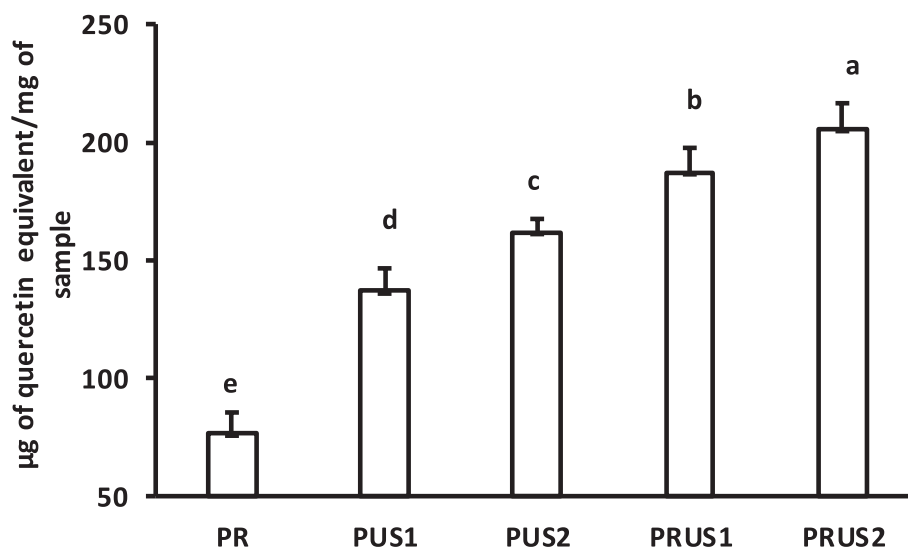


Fig. 3. Total flavonoid content of camel whey-quercetin conjugates prepared using redox-pair (PR); Ultrasonication for 30 min (PUS1); Ultrasonication for 60 min (PUS2); Ultrasonication/redox-pair for 30 min (PRUS1); Ultrasonication /redox-pair for 60 min (PRUS2).

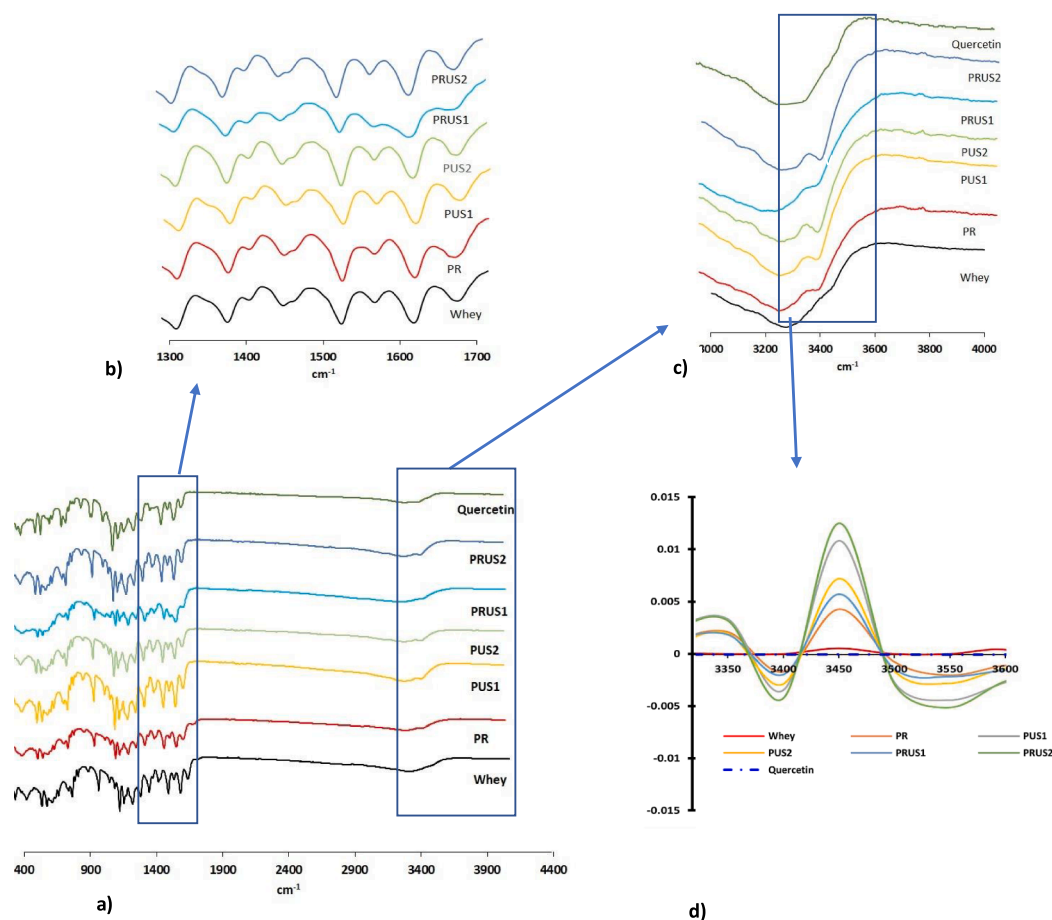


Fig. 4. (a–c) FTIR of camel whey-polyphenol conjugates prepared using redox-pair (PR); Ultrasonication for 30 min (PUS1); Ultrasonication for 60 min (PUS2); Ultrasonication/redox-pair for 30 min (PRUS1); Ultrasonication/redox-pair for 60 min (PRUS2). (d) Second derivative of peak  $3399\text{ cm}^{-1}$  in different whey-quercetin conjugates.

over longer duration of ultrasonication has been previously reported [17]. Small protein aggregates formed are prone to aggregation during longer ultrasonication time [16]. Moreover, there is a significant

increase in the surface hydrophobicity of PUS2 than PUS1 (Table 1) that can act as a driving force for protein agglomeration. Also, a lower negative zeta potential and higher TFC of PUS2 than PUS1 may also

favors particle agglomeration that might increase the overall particle size. Notably when both the treatments were used simultaneously, the particle size decreased significantly in comparison to PUS1 and PUS2. This might be due to break down of whey protein (as seen in SDS-PAGE) into smaller chains resulting in a decrease in the overall particle size.

### 3.1.6. ZETA potential

All the samples including whey proteins as well as whey-quercetin conjugates had negative zeta potential that suggests presence of anionic groups on the surface (Table 1). All whey-quercetin conjugates showed a significant decrease in the zeta potential in comparison to whey ( $P < 0.05$ ). Decrease in zeta potential after the conjugation of whey protein with lotus Proanthocyanidins [14] was also previously reported. Among all the conjugates, PRUS2 and PRUS1 showed highest decrease in the zeta potential possibly due to highest amount of conjugation with quercetin as indicated by TFC in those samples. Lower zeta potential is considered as an advantage as higher negative surface charge will improve the solubility of the complex which is considered as one of the major challenges encountered during whey processing. Conjugates of soy protein and cyanidin-3-galactoside formulated through ultrasonication also showed decreased (more negative) zeta potential in comparison to soy proteins [64]. Thus, ultrasonication can be a novel tool to produce whey-polyphenol conjugates of improved functionality.

### 3.1.7. Surface hydrophobicity

The surface hydrophobicity is an essential physical parameter that influences the functional properties of properties. Conjugation of quercetin with whey protein resulted in a significant decrease in the surface hydrophobicity (Table 1). A decrease in surface hydrophobicity on covalent conjugation of whey with quercetin [46] chlorogenic acid [25] and EGCG [58] was previously reported and attributed to introduction of hydrophilic groups (such as hydroxyl groups) upon conjugation with the phenolic compound. In consent with various previous studies, longer ultrasonication time led to an increase in the surface hydrophobicity of conjugates (PUS1 < PUS2) that can be attributed to exposure of various hydrophobic regions due to breakdown of non-covalent bonds upon increased denaturation [50,51]. Moreover, conjugates produced with ultrasonication/redox-pair method showed a significant decrease in the surface hydrophobicity values. This may be due to higher conjugation in PRUS2 and PRUS1 resulting in a significant increase in the amount of OH groups in the whey protein backbone chain. A decrease in the surface hydrophobicity of soy-protein- cyanidin-3-galactoside conjugates produced using ultrasonication was recently reported [64]. These results further suggest that ultrasonication/redox-pair method may result in higher conjugation of quercetin with whey in comparison to individual techniques.

## 3.2. Functional properties

### 3.2.1. Protein solubility

All whey-protein conjugates showed a significant increase ( $P < 0.05$ ) in the protein solubility in comparison to whey proteins (Table 1). An increase in protein solubility of conjugates has been attributed to increased number of OH groups (due to flavonoid addition) after conjugation. Moreover, increased solubility can also be explained based on decreased surface hydrophobicity and more negative zeta potential in whey-quercetin conjugates that can enhance protein solubilization. Conjugation of whey with quercetin using alkaline method also resulted in increase in the protein solubility at pH > 6 [46]. Covalent conjugation of whey with chlorogenic acid [63] and mulberry polyphenols [28] also resulted in a significant improvement in the protein solubility. In the present study, PUS1 conjugates showed higher solubility than PUS2 as supported by zeta potential and surface hydrophobicity data. The protein solubility in different conjugates was found in the following order: PRUS2 > PRUS1 > PU1 > PU2 > PR suggesting conjugates produced

using ultrasonication as well as ultrasonication/redox-pair method showed better protein solubility than redox-pair method generated conjugates.

### 3.2.2. Foaming properties

Conjugation resulted in a significant improvement in the foaming capacity (FC) of all conjugates in comparison to whey (Fig. 5). An increase in the FC of whey proteins conjugated with chlorogenic acid [63], tannic acid & sodium caseinate [66] and conjugates of egg protein with green tea polyphenol [60] has been reported. Cao, Xiong, Cao, & True, [10] attributed enhanced FC for whey conjugated with gallic acid and EGCG to increased molecular flexibility due to conjugation with the polyphenol. FC is closely related to the rapid diffusion of protein to air–water interface. Introduction of OH groups due to polyphenol addition can facilitate such diffusion at the interface due to increased hydrophilicity of conjugates. The increase in FC was significantly higher in PUS1 and PUS2 in comparison to PRUS1 and PRUS2, indicating US alone was more effective in enhancing FC compared to combined US and free-radical method. Increase in the ultrasonication time increased the FC significantly that can be attributed to the sonication effect on proteins that results in denaturation and reshuffling of hydrophilic balance of the protein molecule in favor of increasing the FC. The FC of PRUS1 and PRUS2 was significantly lower than PUS1 and PUS2 despite of higher level of conjugation as indicated by TFC values. An increase in the concentration of EGCG above an optimum level reduced the FC capacity of whey-EGCG conjugates [10]. An abnormal trend in the FC of egg protein conjugates [60] with increase in the concentration of tea polyphenols and various such discrepancies [47] were previously reported. Higher extent of conjugation can drastically affect the flexibility of conjugates and increase intermolecular repulsion that can adversely affect their filming property at the air–water interface.

Foam stability (FS) of PR, PRUS1 and PRUS2 was significantly lower while PUS1 and PUS2 had significantly higher FS in comparison to whey ( $P < 0.05$ ). Cao et al. [10] reported that whey-EGCG (flavonoid) conjugates had lower foam stability in comparison to whey. However, an increase in the foam stability of covalent conjugates of soy-protein with anthocyanins [57] as well as non-covalent conjugates such as whey-berry polyphenols [49] and lactoferrin-Proanthocyanidins [36] has also been reported. Foam stability of conjugates thus seems to be influenced by the nature and structure of the polyphenol, protein as well as the method of conjugation employed. Higher FS of PUS1 and PUS2 may be attributed to positive effect of ultrasonication at 20 KHz over this treatment range on whey proteins [21]. FS of PUS1 and PUS2 was significantly higher than PRUS1 and PRUS2 that can be attributed to excessive conjugation in ultrasonication/redox-pair method generated conjugates. Higher conjugation is reported to affect the flexibility of proteins as well as lead to steric hinderances at the air-gas interface, thus adversely affects their foaming properties. Also, excessive negative zeta potential of PRUS1 and PRUS2 will hamper the proteins to maintain the air-gas interface stability due to increased repulsion. Moreover, ultrasonication/redox-pair method might lead to hydrolysis of whey proteins (as indicated by the SDS-PAGE) that might further decrease the foam stability as previously reported [31,54].

### 3.2.3. Emulsifying properties

Emulsifying properties of camel whey measured in terms of emulsifying activity index (EAI) and emulsion stability index (ESI) were in the same range as previously reported [33]). All the covalent conjugates showed significantly higher emulsifying properties (Fig. 6). The EAI and ESI of conjugates was found in the order PUS2 > PUS1 > PRUS1 > PR > PRUS2. Increase in the emulsifying properties of conjugates such as whey-EGCG [23] and Duck egg protein hydrolysates-EGCG [44] has been previously reported. Increased emulsifying properties is attributed to the conformational changes induced during covalent conjugation that might lead to the exposure of hydrophobic regions that would facilitate rapid adsorption at the oil water interface [44]. Moreover, increased



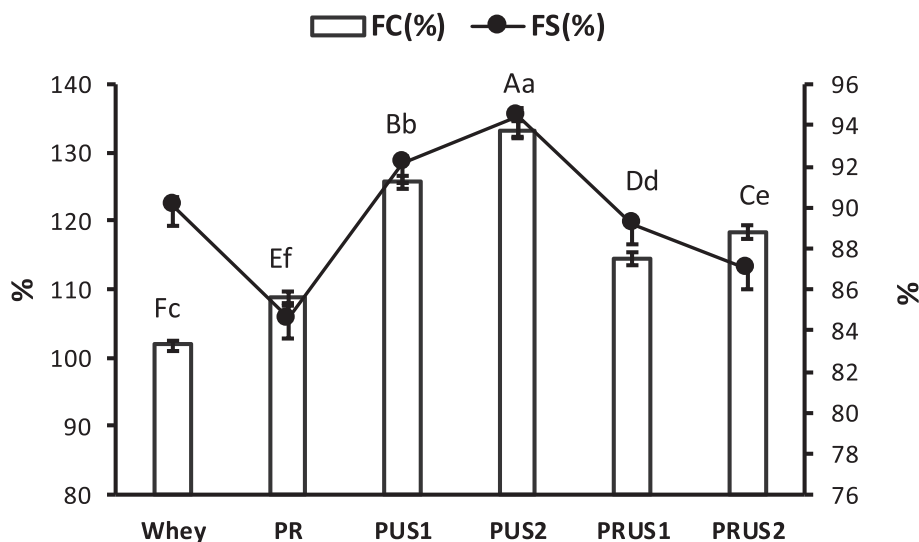


Fig. 5. Foaming properties of camel whey-querctin conjugates prepared using redox-pair (PR); Ultrasonication for 30 min (PUS1); Ultrasonication for 60 min (PUS2); Ultrasonication /redox-pair for 30 min (PRUS1); Ultrasonication/redox-pair for 60 min (PRUS2). Different letters in uppercase indicate a significant difference in Foaming capacity (FC), while different letters in lowercase indicate a significant difference in Foaming stability (FS).

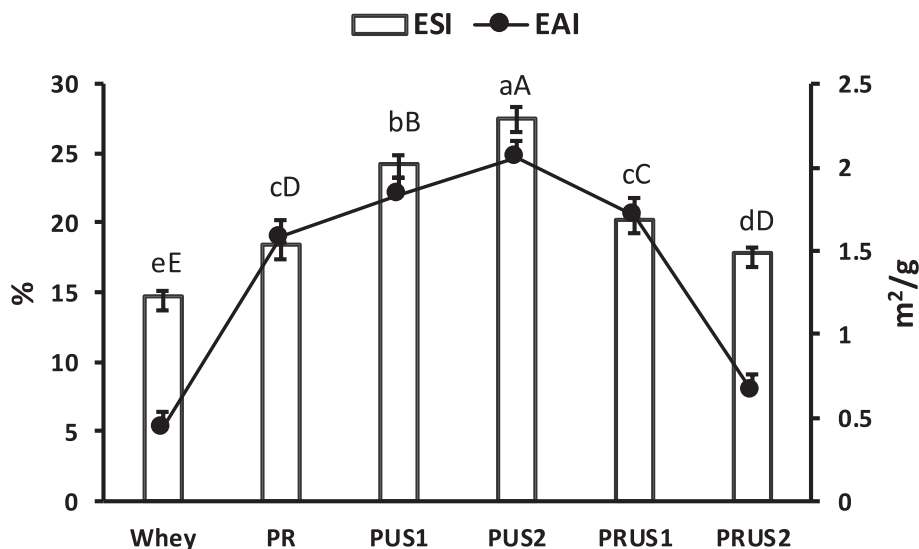


Fig. 6. Emulsifying properties of camel whey-querctin conjugates prepared using redox-pair (PR); Ultrasonication for 30 min (PUS1); Ultrasonication for 60 min (PUS2); Ultrasonication/redox-pair for 30 min (PRUS1); Ultrasonication/redox-pair for 60 min (PRUS2). Different letters in upper case indicate a significant difference in the Emulsion stability index (ESI) while different letters in lower case indicate a significant difference in Emulsion activity index (EAI).

solubility due to increased OH groups in conjugates can further facilitates the transfer of protein to the interfacial regions [25] resulting in improved emulsifying properties. Evidently use of ultrasonication resulted in significantly higher emulsifying properties in comparison to control whey and PR. The ESI of PUS1 and PUS2 increased by 54.39 and 74.19 % in comparison to whey, while 25 and 42% in comparison to PR suggesting ultrasonication was a superior technique for production of conjugates with improved functionality. Jiang et al. [24] reported ultrasonication significantly increased the EAI of allucin-soy conjugates. Furthermore, higher ultrasonication time resulted in higher EAI of PUS2 as previously reported in whey with increase in ultrasonication time [16]. Ultrasonication apart from exposing buried hydrophobic sites can also introduce some polar and non-polar groups leading positive effects on the emulsifying properties of conjugates as reported in egg protein-tea polyphenol conjugates [26]. However, PRUS1 and PRUS2 had significantly lower values of ESI and EAI in comparison to PUS1 and PUS2, yet significantly higher than whey. Ultrasonication/redox-pair

method affected the emulsifying properties of the conjugates possibly due to excessive hydrolysis of protein that is reported to adversely affect the emulsifying properties of whey [31,54] and various other proteins [35]. A decrease in the emulsifying properties of conjugates with high concentration of polyphenol as seen in PRUS1 and PRUS2 might be due to increased steric rigidity that would decreased the protein flexibility and as such the emulsifying property.

### 3.3. Biological activities of whey-querctin conjugates

#### 3.3.1. Antioxidant capacity

The radical scavenging activity of all the samples is depicted in Fig. 7. The DPPH radical scavenging activity of all the conjugates produced in this study was significantly enhanced in comparison to whey protein ( $P < 0.05$ ). This increase can be attributed to addition of OH groups contributed by quercetin molecules after conjugation. Hydroxyl groups (OH) have been linked with hydrogen donating capacity which is

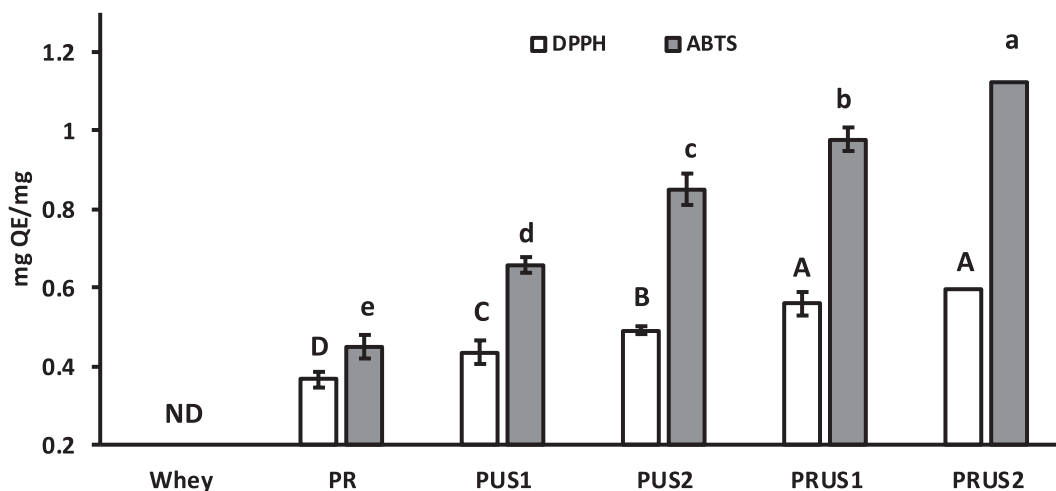


**Fig. 7.** Radical scavenging activity of camel whey-querctin conjugates prepared using redox-pair (PR); Ultrasonication for 30 min (PUS1); Ultrasonication for 60 min (PUS2); Ultrasonication/redox-pair for 30 min (PRUS1); Ultrasonication/redox-pair for 60 min (PRUS2). Quer: Quercetin. ND: Not detected. Different letters on the bars indicate a significant difference between the means.

an important mechanism of antioxidant activity [41]. In comparison to quercetin, the DPPH radical scavenging activity of conjugates significantly decreased ( $P < 0.05$ ). However, the DPPH radical scavenging activity was significantly higher than whey protein as indicated by their higher QEAC values. Previous studies have reported that conjugates generated through free radical method have enhanced antioxidant activity such as  $\beta$ -LG-chlorogenic acid [15] as well as conjugates of lactoferrin with various polyphenols Liu et al., [69]). Moreover, Yi et al. [65] reported that  $\alpha$ -LA (a major camel whey protein) based conjugates had a very high scavenging radical activity that exceeded the control polyphenol. It is noteworthy to mention here that  $\alpha$ -LA is one of the abundant proteins present in camel whey. Among whey-querctin conjugates, those produced by free-radical method (PR) displayed the lowest DPPH (QEAC = 0.366 mg QE/ mg) radical scavenging activities. Other conjugates showed higher DPPH radical scavenging activity compared to PR in the following order: PRUS2 (QEAC = 0.594 mg QE/ mg), PRUS1 (QEAC = 0.558 mg QE/ mg), PUS2 (QEAC = 0.491 mg QE/ mg) and PUS1 (QEAC = 0.435 mg QE/ mg). A similar trend was seen in ABTS radical scavenging activity of conjugates with no activity detected in whey. Among conjugates, lowest ABTS radical scavenging activity was reported for PR (QEAC = 0.445 mg QE/ mg) while PUS1 (QEAC = 0.652 mg QE/ mg) and PUS2 (QEAC = 0.857 mg QE/ mg) showed significantly higher ABTS radical scavenging activity ( $P < 0.05$ ) compared to PR. The highest ABTS scavenging activity was found in ultrasonication/redox-pair generated conjugates: PRUS1 (QEAC = 0.971 mg QE/ mg) and PRUS2 (QEAC = 1.021 mg QE/ mg) ( $P < 0.05$ ). Thus, ultrasonication as well as ultrasonication/redox-pair methods generated conjugates with higher antioxidant activity in comparison to conjugates produced using redox-pair method. The higher antioxidant activity of PUS1 & PUS2 as well as PRUS1 & PRUS2 in comparison to PR can be attributed to the presence of both covalently as well as non-covalently conjugated polyphenols as previously reported in soy protein isolates [64]. Moreover, Wei et al. [58] reported that non-covalently bonded polyphenol fraction had higher radical scavenging activity when same masses of covalently bound polyphenols. Conjugates PRUS1 and PRUS2 showed the highest antioxidant activity in comparison to other conjugates that may be attributed to their higher total flavonoid (quercetin) content. Also, it cannot be ignored that there might be some level of whey protein hydrolysis caused by combination of ultrasonication and redox pair methods as indicated by the SDS-PAGE that might produce various bioactive peptides with high antioxidant activity. However, such a claim needs further investigation.

### 3.3.2. Antidiabetic and anti-obesity properties of whey-querctin conjugates

**3.3.2.1.  $\alpha$ -Glucosidase and DPP-IV inhibition.** Antidiabetic property of conjugates was explored by studying the inhibitory effect of conjugates against various metabolic enzymatic markers such as  $\alpha$ -glucosidase and DPP-IV that are essential in regulating blood glucose levels. There is no existing literature about the inhibition of DPP-IV and  $\alpha$ -glucosidase by any whey-polyphenol conjugates produced till date. The  $\alpha$ -glucosidase inhibition (AGI) and DPP-IV inhibition potential (DIP) of whey, quercetin and whey-querctin conjugates is shown in Fig. 8(a & b). All whey-querctin conjugates showed high level of AGI while no inhibition could be detected at the same concentration of whey (5  $\mu$ g/ml). However, an increase in the concentration of whey to 5 mg/ml showed 35% inhibition of  $\alpha$ -glucosidase (Data not shown). Notably the AGI of conjugates was significantly lower than quercetin. Higher AGI potential of whey-protein conjugates in comparison to whey can be attributed to the conjugation of quercetin, which has been reported for its tendency to form hydrogen bonds with the catalytic triad (Asp214, Glu 276 and Asp 349) located in the active site of  $\alpha$ -glucosidase [43]). Evidently the hydrogen bond forming capacity of conjugates increases notably after conjugation (as depicted by the FTIR) due to addition of hydroxyl groups through quercetin addition that can lead to increased AGI. Interestingly, the hydrogen atom transfer (HAT) value of quercetin in water is lowest for 3-OH (C-Ring) [67] suggesting possibility of conjugation at C ring of quercetin. This will result in availability of 3'-OH (forms two hydrogen bonds with the Glu 276) as well as 4'-OH (hydrogen bonds with Asp 349) of the B-ring which are strongly involved in AGI [48,62]. The binding of whey at C-ring of quercetin may also explain the significant decrease of AGI of conjugates in comparison to quercetin as previously explained during C-ring substitution of quercetin [43]. However, the exact binding site of polyphenol at which protein is conjugated [38] and the site where the conjugate binds with the enzyme are not clear yet and need further exploration.

DPP-IV inhibitors are an emerging class of therapeutic drugs for managing diabetes. DPP-IV inhibition was not detected in whey. Conjugation significantly improved the DPP-IV inhibition of whey that can be attributed to DPP-IV inhibitory property of quercetin attached with the whey protein. Interestingly whey displayed no DPP-IV inhibition even when the concentration of whey was increased to 5 mg/ml (Data not shown). DPP-IV inhibition of quercetin is attributed to five hydrogen bonds with Val 738, Ser 720, Tyr 700, Ala 732 and Met 733 [53] and introduction of OH in whey protein due to quercetin addition facilitates formation of various linkages between the active site of

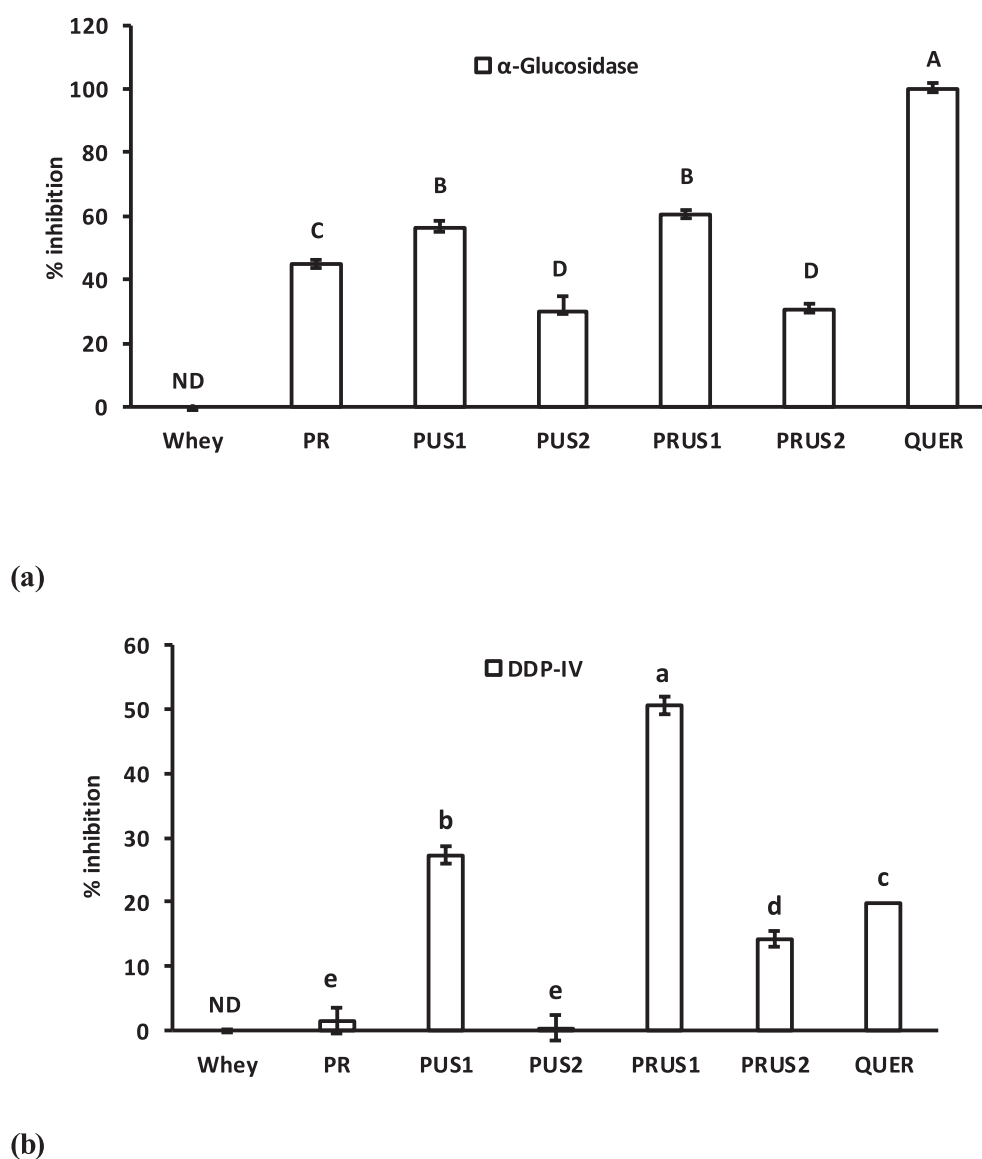


**Fig. 8.** (a)  $\alpha$ -glucosidase and (b) DPP-IV Inhibitory potential of camel whey-quercetin conjugates prepared using redox-pair (PR); Ultrasonication for 30 min (PUS1); Ultrasonication for 60 min (PUS2); Ultrasonication/redox-pair for 30 min (PRUS1); Ultrasonication/redox-pair for 60 min (PRUS2). Quer: Quercetin. ND: Not detected. Different letters on the bars indicate a significant difference between the means.

enzyme and the conjugates. Interestingly, the DPP-IV inhibition of PRUS1 was significantly higher than pure quercetin molecule and should be studied further.

Conjugates produced at lower ultrasonication time showed superior AGI and DPP-IV inhibition in comparison to conjugates produced at higher ultrasonication time (PUS1 > PUS2). Notably quercetin has been reported to show competitive inhibition against various metabolic enzymes such as  $\alpha$ -glucosidase [43] which emphasizes the importance of the size that would fit in the active site without any steric hinderances. Interestingly the particle size of the conjugates at longer ultrasonication time (PUS2 and PRUS2) is larger that might offer higher steric hinderance between the enzyme and inhibitor, thereby decreasing the enzyme inhibiting potential. Moreover, an increase in the ultrasonication time decreased the extent of hydrogen bonding capacity of conjugates (FTIR results; Fig. 4) which may be another possible reason for reduced enzyme inhibiting potential. Overall, conjugation of whey proteins with quercetin resulted in generation of strong DPP-IV and  $\alpha$ -glucosidase inhibition potential with superior outcome obtained when conjugation was achieved with the intervention of ultrasonication.

**3.3.2.2. Cholesterol esterase and lipase inhibition.** *In-vitro* anti-obesity potential of conjugates was reported in terms of the inhibiting capacity of conjugates against cholesterol esterase and lipase, crucial enzyme markers involved in fat metabolism (Fig. 9). There is no literature available about the cholesterol esterase inhibition (CEI) by any protein-polyphenol conjugate till date. CE is a pancreatic enzyme present in bile that catalyzes the release of cholesterol and free fatty acids from dietary cholesterol esters. As such, CEI can slowdown cholesterol uptake by human body indirectly by decreasing the level of cholesterol produced from dietary lipids. The conjugates showed high level of CEI which was not detected in case of whey when tested a concentration (5  $\mu$ g/ml). Moreover, different concentrations of whey protein were tested and it was found that whey proteins displayed  $\approx$ 50% inhibition at 5 mg/ml (Not presented here). The CEI of whey-quercetin conjugates was lower than quercetin alone except PRUS1 that showed complete inhibition of cholesterol esterase. Notably there was a non-significant difference in the CEI of PR, PUS1 and PRUS2 conjugates. The CEI of quercetin has been associated with its structural attributes and proceeds through uncompetitive inhibition [55]. This points towards the irregular trend obtained during CEI by conjugates needs further in-depth studies

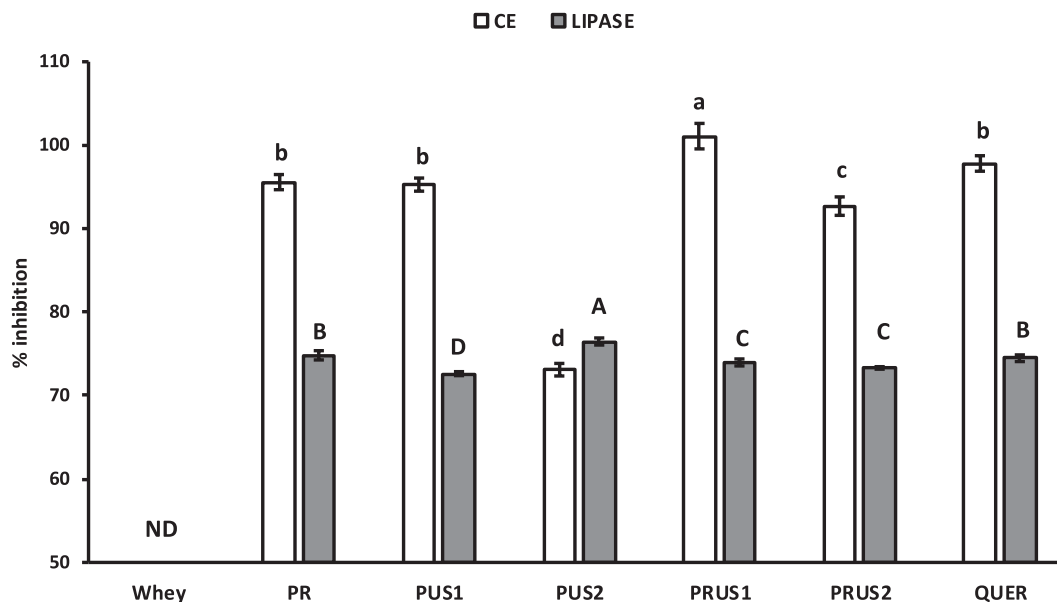


**Fig. 9.** % Inhibition of Cholesterol esterase (CE) by camel whey-quercetin conjugates prepared using redox-pair (PR); Ultrasonication for 30 min (PUS1); Ultrasonication for 60 min (PUS2); Ultrasonication/redox-pair for 30 min (PRUS1); Ultrasonication/redox-pair for 60 min (PRUS2). Quer: Quercetin, ND: Not detected. Quer: Quercetin. ND: Not detected. Different letters on the bars indicate a significant difference between the means.

related to the mechanism of inhibition of CE by whey-protein conjugates.

Unlike whey proteins, whey-quercetin conjugates showed high level of pancreatic lipase inhibition (PLI) (Fig. 9). The increase in lipase inhibiting potential of conjugates in comparison to whey may be attributed to conjugation of quercetin with the whey proteins. Quercetin has been previously reported for lipase inhibiting potential that is attributed to its ability to interact with the enzyme [8]. Wu et al. [59] also reported that quercetin-3 rhamnoside can enter the hydrophobic cavity and form hydrogen bonds with Ser153 and His264 near the active site of lipase. Although all conjugates showed superior PLI than whey, a mixed trend in the PLI of conjugates was seen. Notably PUS2 showed significantly higher inhibition while rest of the conjugates showed significantly lower lipase inhibition in comparison to control quercetin. The linkage site as well as the ring of quercetin that is linked to whey in conjugates that may significantly affect their inhibition potential has not been clearly established so far. Derivates of quercetin have been reported to have varying degrees of lipase inhibiting potential. For example, galloylation of various flavonoids such as quercitrin, EGCG, epicatechin gallate was reported to enhance lipase inhibition while glycosylation at 3-hydroxyl group was reported to decreased it [52]. The authors also reported a variation in OH groups around the quercetin backbone affects the lipase inhibition. As such different methods with different levels of quercetin binding as well as possibility of different linkage points of quercetin with whey may result in different inhibiting efficiencies. Moreover, different conjugates showed different extent of OH group influences in their FTIR suggesting varied capacities of the conjugate to interact with the target enzyme. Thus, further in-depth studies related to enzyme inhibition by whey-quercetin conjugates is highly recommended.

#### 4. Conclusion

Ultrasonication turns out to be an efficient method for production of camel whey-quercetin conjugates in comparison to redox-pair method by reducing the production time. While redox pair generated conjugates are linked principally through covalent linkages, samples generated through ultrasonication involve both covalent as well as non-covalent linkages. Conjugates produced using ultrasonication had superior

techno-functional and bioactive properties especially anti-diabetic and anti-obesity potential in comparison to pure whey proteins and redox-pair generated conjugates. A conjoint application of redox pair and ultrasonication in comparison to individual treatments further improved the bioactive properties of conjugates but adversely affected some of the techno-functional properties. The mechanism of conjugation through ultrasonication needs further in-depth studies to understand variation in bioactivities in particular the enzyme inhibiting potential of conjugates. Incorporation of these multifunctional ingredients for production of functional foods and their survival during processing is also recommended.

#### CRediT authorship contribution statement

**Waqas N. Baba:** Conceptualization, Methodology, Formal analysis, Validation, Investigation, Writing – original draft. **Raghad Abdel Rahman:** Investigation, Methodology. **Sajid Maqsood:** Conceptualization, Funding acquisition, Methodology, Validation, Writing – review & editing, Supervision.

#### Declaration of Competing Interest

The authors declare that they have no known competing financial interests or personal relationships that could have appeared to influence the work reported in this paper.

#### Acknowledgement

We would like to thank the UAE University for funding this research through PhD research grant (31F155) and UPAR grant (31F094).

#### Appendix A. Supplementary data

Supplementary data to this article can be found online at <https://doi.org/10.1016/j.ultsonch.2021.105784>.

#### References

- [1] M. Ahmad, P. Mudgil, A. Gani, F. Hamed, F.A. Masoodi, S. Maqsood, Nano-encapsulation of catechin in starch nanoparticles: Characterization, release

- behavior and bioactivity retention during simulated in-vitro digestion, *Food Chem.* 270 (2019) 95–104. <https://doi.org/10.1016/j.foodchem.2018.07.024>.
- [2] M. Ahmad, P. Mudgil, S. Maqsood, Camel whey protein microparticles for safe and efficient delivery of novel camel milk derived probiotics, *LWT* 108 (2019) 81–88. <https://doi.org/10.1016/j.lwt.2019.03.008>.
- [3] W.N. Baba, B. Baby, P. Mudgil, C.-Y. Gan, R. Vijayan, S. Maqsood, Pepsin generated camel whey protein hydrolysates with potential antihypertensive properties: Identification and molecular docking of antihypertensive peptides, *LWT* 143 (2021) 111135. <https://doi.org/10.1016/j.lwt.2021.111135>.
- [4] W.N. Baba, S. Din, H.A. Punoo, T.A. Wani, M. Ahmad, F.A. Masoodi, Comparison of cheese and paneer whey for production of a functional pineapple beverage: Nutrachemical properties and Shelf life, *J. Food Sci. Technol.* 53 (6) (2016) 2558–2568.
- [5] W.N. Baba, D.J. McClements, S. Maqsood, Whey protein-polyphenol conjugates and complexes: Production, characterization, and applications, *Food Chem.* 365 (2021) 130455. <https://doi.org/10.1016/j.foodchem.2021.130455>.
- [6] W.N. Baba, P. Mudgil, B. Baby, R. Vijayan, C.-Y. Gan, S. Maqsood, New insights into the cholesterol esterase- and lipase-inhibiting potential of bioactive peptides from camel whey hydrolysates: identification, characterization, and molecular interaction, *J. Dairy Sci.* 104 (7) (2021) 7393–7405. <https://doi.org/10.3168/jds.2020-19868>.
- [7] W.N. Baba, P. Mudgil, H. Kamal, B.P. Kilari, C.-Y. Gan, S. Maqsood, Identification and characterization of novel  $\alpha$ -amylase and  $\alpha$ -glucosidase inhibitory peptides from camel whey proteins, *J. Dairy Sci.* 104 (2) (2021) 1364–1377. <https://doi.org/10.3168/jds.2020-19271>.
- [8] A.-S. Bustos, A. Håkansson, J.A. Linares-Pastén, J.M. Peñarrieta, L. Nilsson, O. Chen, Interaction of quercetin and epigallocatechin gallate (EGCG) aggregates with pancreatic lipase under simplified intestinal conditions, *PLoS ONE* 15 (4) (2020) e0224853. <https://doi.org/10.1371/journal.pone.0224853>.
- [9] Y. Cao, Y.L. Xiong, Interaction of whey proteins with phenolic derivatives under neutral and acidic pH conditions, *J. Food Sci.* 82 (2) (2017) 409–419.
- [10] Y. Cao, Y.L. Xiong, Y. Cao, A.D. True, Interfacial properties of whey protein foams as influenced by preheating and phenolic binding at neutral pH, *Food Hydrocolloids* 82 (2018) 379–387.
- [11] P. Chanphai, H.A. Tajmir-Riahi, Tea polyphenols bind serum albumins: A potential application for polyphenol delivery, *Food Hydrocolloids* 89 (2019) 461–467.
- [12] I. Chelph, P. Gatellier, V. Santé-Lhoutellier, A simplified procedure for myofibril hydrophobicity determination, *Meat Sci.* 74 (4) (2006) 681–683.
- [13] Y. Chen, F. Huang, B. Xie, Z. Sun, D.J. McClements, Q. Deng, Fabrication and characterization of whey protein isolates-lotus seedpod proanthocyanin conjugate: Its potential application in oxidizable emulsions, *Food Chem.* 346 (2021), 128680.
- [14] Y. Chen, R. Zhang, B. Xie, Z. Sun, D.J. McClements, Lotus seedpod proanthocyanidin-whey protein complexes: Impact on physical and chemical stability of  $\beta$ -carotene-nanoemulsions, *Food Res. Int.* 127 (2020) 108738. <https://doi.org/10.1016/j.foodres.2019.108738>.
- [15] Y. Fan, Y. Zhang, W. Yokoyama, J. Yi,  $\beta$ -Lactoglobulin-chlorogenic acid conjugate-based nanoparticles for delivery of (–)-epigallocatechin-3-gallate, *RSC Adv.* 7 (35) (2017) 21366–21374.
- [16] H. Gao, L. Ma, T. Li, D. Sun, J. Hou, A. Li, Z. Jiang, Impact of ultrasonic power on the structure and emulsifying properties of whey protein isolate under various pH conditions, *Process Biochem.* 81 (2019) 113–122.
- [17] İ. Gülseren, D. Güzey, B.D. Bruce, J. Weiss, Structural and functional changes in ultrasonicated bovine serum albumin solutions, *Ultrason. Sonochem.* 14 (2) (2007) 173–183.
- [18] Y. Hailu, E.B. Hansen, E. Seifu, M. Eshetu, R. Ipsen, S. Kappeler, Functional and technological properties of camel milk proteins: a review, *J. Dairy Res.* 83 (4) (2016) 422–429.
- [19] T.J. Herald, P. Gadgil, M. Tilley, High-throughput micro plate assays for screening flavonoid content and DPPH-scavenging activity in sorghum bran and flour, *J. Sci. Food Agric.* 92 (11) (2012) 2326–2331.
- [20] S. Jafar, H. Kamal, P. Mudgil, H.M. Hassan, S. Maqsood, Camel whey protein hydrolysates displayed enhanced cholesterol esterase and lipase inhibitory, anti-hypertensive and anti-haemolytic properties, *LWT* 98 (2018) 212–218.
- [21] A.R. Jambrak, T.J. Mason, V. Lelas, Z. Herceg, I.L. Herceg, Effect of ultrasound treatment on solubility and foaming properties of whey protein suspensions, *J. Food Eng.* 86 (2) (2008) 281–287.
- [22] A.R. Jambrak, T.J. Mason, V. Lelas, L. Paniwnyk, Z. Herceg, Effect of ultrasound treatment on particle size and molecular weight of whey proteins, *J. Food Eng.* 121 (2014) 15–23. <https://doi.org/10.1016/j.jfoodeng.2013.08.012>.
- [23] Z. Jia, M. Zheng, F. Tao, W. Chen, G. Huang, J. Jiang, Effect of covalent modification by (–)-epigallocatechin-3-gallate on physicochemical and functional properties of whey protein isolate, *LWT-Food Sci. Technol.* 66 (2016) 305–310.
- [24] H. Jiang, Z. Xing, Y. Wang, Z. Zhang, B. Kumah Mintah, M. Dabbour, Y. Li, R. He, L. Huang, H. Ma, Preparation of allixin-whey protein isolate conjugates: Allixin extraction by water, conjugates' ultrasound-assisted binding and its stability, solubility and emulsibility analysis, *Ultrason. Sonochem.* 63 (2020) 104981. <https://doi.org/10.1016/j.ultrsonch.2020.104981>.
- [25] J. Jiang, Z. Zhang, J. Zhao, Y. Liu, The effect of non-covalent interaction of chlorogenic acid with whey protein and casein on physicochemical and radical-scavenging activity of in vitro protein digests, *Food Chem.* 268 (2018) 334–341. <https://doi.org/10.1016/j.foodchem.2018.06.015>.
- [26] H. Jing, J. Sun, Y. Mu, M. Obadi, D.J. McClements, B. Xu, Sonochemical effects on the structure and antioxidant activity of egg white protein-tea polyphenol conjugates, *Food Funct.* 11 (8) (2020) 7084–7094.
- [27] H. Kamal, S. Jafar, P. Mudgil, C. Murali, A. Amin, S. Maqsood, Inhibitory properties of camel whey protein hydrolysates toward liver cancer cells, dipeptidyl peptidase-IV, and inflammation, *J. Dairy Sci.* 101 (10) (2018) 8711–8720.
- [28] I. Khalifa, J. Peng, Y. Jia, J. Li, W. Zhu, X.u. Yu-juan, C. Li, Anti-glycation and anti-hardening effects of microencapsulated mulberry polyphenols in high-protein-sugar ball models through binding with some glycation sites of whey proteins, *Int. J. Biol. Macromol.* 123 (2019) 10–19.
- [29] A.B. Khatkar, A. Kaur, S.K. Khatkar, N. Mehta, Characterization of heat-stable whey protein: Impact of ultrasound on rheological, thermal, structural and morphological properties, *Ultrason. Sonochem.* 49 (2018) 333–342.
- [30] J. Królczyk, T. Dawidziuk, E. Janiszewska-Turak, B. Sotowiej, Use of whey and whey preparations in the food industry—a review, *Polish J. Food Nutr. Sci.* 66 (3) (2016) 157–165.
- [31] C.A. KUEHLER, C.M. STINE, Effect of enzymatic hydrolysis on some functional properties of whey protein, *J. Food Sci.* 39 (2) (1974) 379–382.
- [32] R. Lajnaf, H. Gharsallah, H. Attia, M.A. Ayadi, Comparative study on antioxidant, antimicrobial, emulsifying and physico-chemical properties of purified bovine and camel  $\beta$ -casein, *LWT* 140 (2021) 110842. <https://doi.org/10.1016/j.lwt.2020.110842>.
- [33] R. Lajnaf, I. Trigui, O. Samet-Bali, H. Attia, M.A. Ayadi, Comparative study on emulsifying and physico-chemical properties of bovine and camel acid and sweet wheys, *J. Food Eng.* 268 (2020) 109741. <https://doi.org/10.1016/j.jfoodeng.2019.109741>.
- [34] L.C. Laleye, B. Jobe, A.A.H. Wasesa, Comparative study on heat stability and functionality of camel and bovine milk whey proteins, *J. Dairy Sci.* 91 (12) (2008) 4527–4534.
- [35] G. Leni, L. Soeteman, A. Caligiani, S. Sforza, L. Bastiaens, Degree of hydrolysis affects the techno-functional properties of lesser mealworm protein hydrolysates, *Foods* 9 (4) (2020) 381.
- [36] C. Li, T. Dai, J. Chen, X. Li, T. Li, C. Liu, D.J. McClements, Protein-polyphenol functional ingredients: The foaming properties of lactoferrin are enhanced by forming complexes with procyanidin, *Food Chem.* 339 (2021), 128145.
- [37] F. Liu, D.i. Wang, C. Ma, Y. Gao, Conjugation of polyphenols prevents lactoferrin from thermal aggregation at neutral pH, *Food Hydrocolloids* 58 (2016) 49–59.
- [38] J. Liu, H. Yong, X. Yao, H. Hu, D. Yun, L. Xiao, Recent advances in phenolic-protein conjugates: synthesis, characterization, biological activities and potential applications, *RSC Adv.* 9 (61) (2019) 35825–35840.
- [39] G. Liu, Q. Zhong, Glycation of whey protein to provide steric hindrance against thermal aggregation, *J. Agric. Food Chem.* 60 (38) (2012) 9754–9762.
- [40] S. Maqsood, A. Al-Dowaila, P. Mudgil, H. Kamal, B. Jobe, H.M. Hassan, Comparative characterization of protein and lipid fractions from camel and cow milk, their functionality, antioxidant and antihypertensive properties upon simulated gastro-intestinal digestion, *Food Chem.* 279 (2019) 328–338. <https://doi.org/10.1016/j.foodchem.2018.12.011>.
- [41] S. Maqsood, S. Benjakul, Comparative studies of four different phenolic compounds in vitro antioxidant activity and the preventive effect on lipid oxidation of fish oil emulsion and fish mince, *Food Chem.* 119 (1) (2010) 123–132.
- [42] I.B. O'Loughlin, P.M. Kelly, B.A. Murray, R.J. FitzGerald, A. Brodtkorb, Concentrated whey protein ingredients: A Fourier transformed infrared spectroscopy investigation of thermally induced denaturation, *Int. J. Dairy Technol.* 68 (3) (2015) 349–356.
- [43] C. Proença, M. Freitas, D. Ribeiro, E.F.T. Oliveira, J.L.C. Sousa, S.M. Tomé, M. J. Ramos, A.M.S. Silva, P.A. Fernandes, E. Fernandes,  $\alpha$ -Glucosidase inhibition by flavonoids: an in vitro and in silico structure-activity relationship study, *J. Enzyme Inhib. Med. Chem.* 32 (1) (2017) 1216–1228.
- [44] T.H. Qian, S. Benjakul, Duck egg albumen hydrolysate-epigallocatechin gallate conjugates: Antioxidant, emulsifying properties and their use in fish oil emulsion, *Colloids Surf., A* 579 (2019), 123711.
- [45] H.M. Rawel, D. Czajka, S. Rohn, J. Kroll, Interactions of different phenolic acids and flavonoids with soy proteins, *Int. J. Biol. Macromol.* 30 (3-4) (2002) 137–150.
- [46] H.M. Rawel, S. Rohn, J. Kroll, Influence of a sugar moiety (rhamnosylglucoside) at 3-O position on the reactivity of quercetin with whey proteins, *Int. J. Biol. Macromol.* 32 (3-5) (2003) 109–120.
- [47] S.D. Rodríguez, M. von Staszewski, A.M.R. Pilosof, Green tea polyphenols-whey proteins nanoparticles: Bulk, interfacial and foaming behavior, *Food Hydrocolloids* 50 (2015) 108–115.
- [48] Sarian, M. N., Ahmed, Q. U., Mat So'ad, S. Z., Alhassan, A. M., Murugesu, S., Perumal, V., . . . Latip, J. (2017). Antioxidant and antidiabetic effects of flavonoids: A structure-activity relationship based study. *BioMed research international*, 2017.
- [49] M. Schneider, D. Esposito, M.A. Lila, E.A. Foegeding, Formation of whey protein-polyphenol meso-structures as a natural means of creating functional particles, *Food Funct.* 7 (3) (2016) 1306–1318.
- [50] X. Shen, T. Fang, F. Gao, M. Guo, Effects of ultrasound treatment on physicochemical and emulsifying properties of whey proteins pre-and post-thermal aggregation, *Food Hydrocolloids* 63 (2017) 668–676.
- [51] X. Shen, S. Shao, M. Guo, Ultrasound-induced changes in physical and functional properties of whey proteins, *Int. J. Food Sci. Technol.* 52 (2) (2017) 381–388.
- [52] S. Shimura, Y. Itoh, A. Yamashita, A. Kitano, T. Hatano, T. Yoshida, T. Okuda, Inhibitory effects of flavonoidson lipase, *Nippon Shokuhin Kogyo Gakkaishi* 41 (11) (1994) 847–850.
- [53] A.-K. Singh, P.K. Patel, K. Choudhary, J. Joshi, D. Yadav, J.-O. Jin, Quercetin and coumarin inhibit Dipeptidyl Peptidase-IV and exhibits antioxidant properties: in silico, in vitro, ex vivo, *Biomolecules* 10 (2) (2020) 207.
- [54] R. Sinha, C. Radha, J. Prakash, P. Kaul, Whey protein hydrolysate: Functional properties, nutritional quality and utilization in beverage formulation, *Food Chem.* 101 (4) (2007) 1484–1491.

- [55] Sivashanmugam, T., Muthukrishnan, S., Umamaheswari, M., Asokkumar, K., Subhadradevi, V., Jagannath, P., & Madeswaran, A. Cholesterol esterase inhibitory activity of flavonoids using in silico and in vitro studies.
- [56] U.G. Spizzirri, F. Iemma, F. Puoci, G. Cirillo, M. Curcio, O.I. Parisi, N. Picci, Synthesis of antioxidant polymers by grafting of gallic acid and catechin on gelatin, *Biomacromolecules* 10 (7) (2009) 1923–1930.
- [57] X. Sui, H. Sun, B. Qi, M. Zhang, Y. Li, L. Jiang, Functional and conformational changes to soy proteins accompanying anthocyanins: Focus on covalent and non-covalent interactions, *Food Chem.* 245 (2018) 871–878.
- [58] Z. Wei, W. Yang, R. Fan, F. Yuan, Y. Gao, Evaluation of structural and functional properties of protein-EGCG complexes and their ability of stabilizing a model  $\beta$ -carotene emulsion, *Food Hydrocolloids* 45 (2015) 337–350.
- [59] D. Wu, R. Duan, L. Tang, X. Hu, F. Geng, Q. Sun, H. Li, Binding mechanism and functional evaluation of quercetin 3-rhamnoside on lipase, *Food Chem.* 359 (2021), 129960.
- [60] W. Wu, M. Clifford, N.K. Howell, The effect of instant green tea on the foaming and rheological properties of egg albumen proteins, *J. Sci. Food Agric.* 87 (10) (2007) 1810–1819.
- [61] X. Wu, Y. Lu, H. Xu, D. Lin, Z. He, H. Wu, L. Liu, Z. Wang, Reducing the allergenic capacity of  $\beta$ -lactoglobulin by covalent conjugation with dietary polyphenols, *Food Chem.* 256 (2018) 427–434.
- [62] H. Xu, Inhibition kinetics of flavonoids on yeast  $\alpha$ -glucosidase merged with docking simulations, *Protein Pept. Lett.* 17 (10) (2010) 1270–1279.
- [63] H. Xu, T. Zhang, Y. Lu, X. Lin, X. Hu, L. Liu, Z. He, X. Wu, Effect of chlorogenic acid covalent conjugation on the allergenicity, digestibility and functional properties of whey protein, *Food Chem.* 298 (2019) 125024, <https://doi.org/10.1016/j.foodchem.2019.125024>.
- [64] F. Xue, C. Li, B. Adhikari, Physicochemical properties of soy protein isolates-cyanidin-3-galactoside conjugates produced using free radicals induced by ultrasound, *Ultrason. Sonochem.* 64 (2020) 104990, <https://doi.org/10.1016/j.ultsonch.2020.104990>.
- [65] J. Yi, Y. Fan, Y. Zhang, L. Zhao, Characterization of catechin- $\alpha$ -lactalbumin conjugates and the improvement in  $\beta$ -carotene retention in an oil-in-water nanoemulsion, *Food Chem.* 205 (2016) 73–80.
- [66] F. Zhan, Y. Chen, J. Hu, M. Youssef, A. Korin, J. Li, B. Li, Combining surface dilatational rheology and quantitative proteomics as a tool for understanding microstructures of air/water interfaces stabilized by sodium caseinate/tannic acid complex, *Food Hydrocolloids* 102 (2020) 105627, <https://doi.org/10.1016/j.foodhyd.2019.105627>.
- [67] Y.-Z. Zheng, G. Deng, Q. Liang, D.-F. Chen, R. Guo, R.-C. Lai, Antioxidant activity of quercetin and its glucosides from propolis: a theoretical study, *Sci. Rep.* 7 (1) (2017) 1–11.
- [68] A. Zouari, R. Lajnaf, C. Lopez, P. Schuck, H. Attia, M.A. Ayadi, Physicochemical, techno-functional, and fat melting properties of spray-dried camel and bovine milk powders, *J. Food Sci.* 86 (1) (2021) 103–111.
- [69] Fuguo Liu, et al., Structural characterization and functional evaluation of lactoferrinpolyphenol conjugates formed by free-radical graft copolymerization, *RCS Advances* 5 (20) (2015) 15641–15651.